ORIGINAL RESEARCH

American Society of Plant Biologists | S E B SOCIETY FOR EXPERIMENTAL BIOLOGY | WILEY

Using CRL3^{BPM} E3 ligase substrate recognition sites as tools to impact plant development and stress tolerance in *Arabidopsis thaliana*

Raed Al-Saharin[1,2] | Sutton Mooney[1] | Nico Dissmeyer[3] | Hanjo Hellmann[1]

[1]Washington State University, Pullman, Washington, USA

[2]Tafila Technical University, Tafila, Jordan

[3]Department of Plant Physiology and Protein Metabolism Lab, University of Osnabruck, Osnabruck, Germany

Correspondence
Hanjo Hellmann, Washington State University, Pullman, WA, USA.
Email: hellmann@wsu.edu

Abstract

Cullin-based RING E3 ligases that use BTB/POZ-MATH (BPM) proteins as substrate receptors have been established over the last decade as critical regulators in plant development and abiotic stress tolerance. As such they affect general aspects of shoot and root development, flowering time, embryo development, and different abiotic stress responses, such as heat, drought and salt stress. To generate tools that can help to understand the role of CRL3^{BPM} E3 ligases in plants, we developed a novel system using two conserved protein-binding motifs from BPM substrates to transiently block CRL3^{BPM} activity. The work investigates *in vitro* and *in planta* this novel approach, and shows that it can affect stress tolerance in plants as well as developmental aspects. It thereby can serve as a new tool for studying this E3 ligase in plants.

KEYWORDS
Arabidopsis, BPM, CRL3, development, E3 ligase, N-degron, stress, ubiquitin

1 | INTRODUCTION

Plants are highly dependent on flexible cellular pathways to react and cope with changes in their environment. This is critical for coordinating and balancing developmental progress with potentially detrimental growth conditions. With predicted global climate changes and an increasing world population, it becomes imperative to develop new strategies that allow crop plants to maintain high yields in order to retain sustainable agriculture.

E3 ligases may represent ideal tools to generate more robust crop plants that tolerate better abiotic stress conditions while still generating high yields. E3 ligases are key regulators within the ubiquitin proteasome pathway, and they control protein stability through targeted attachment of ubiquitin moieties on selected substrate proteins (Chen & Hellmann, 2013). Such marked proteins are often

degraded by the 26S proteasome, representing a critical step to trigger cellular responses. Because ubiquitylation and degradation of a protein can occur within minutes after a stimulating signal, E3 ligases provide an essential feature to permit fast reactions in response to changing environmental conditions (Chen & Hellmann, 2013).

The E3 ligase this work focuses on is a multimeric protein complex that consists of a Cullin 3 (CUL3) protein as a scaffolding subunit, which binds at its C-terminal region a RING-finger protein, RBX1, and at its N-terminal region proteins that contain a Broad-Complex, Tramtrack and Bric a brac/POxvirus and Zinc finger (BTB/POZ) domain (Figueroa et al., 2005; Weber et al., 2005). The E3 ligase is highly conserved among eukaryotes and is generally referred to as CUL3-RING-E3 ligase (CRL3) (Choi et al., 2014).

Arabidopsis thaliana encodes for 80 BTB/POZ domain containing proteins (Gingerich et al., 2007), though for most of these an

association with CUL3 has not yet been described. One BTB/POZ subfamily has an additional Meprin And Traf Homology (MATH) domain, which is required for binding specific CRL3[BPM] substrates (Chen et al., 2013, 2015; Chico et al., 2020; Lechner et al., 2011; Mooney et al., 2019; Morimoto et al., 2017; Weber & Hellmann, 2009). In Arabidopsis, this subfamily comprises six members that are generally referred to as BTB/POZ-MATH (BPM) proteins (Weber et al., 2005).

Most BPM substrates described so far are members of four different transcription factor families: Ethylene Response Factor/Apetala2 (ERF/AP2) (Chen et al., 2013; Mooney et al., 2019; Weber & Hellmann, 2009), MYB R2R3 domain proteins (MYB) (Chen et al., 2015), Homeodomain leucine zipper class I/Homeobox (Hd-Zip/HB) (Lechner et al., 2011), and very recently also MYC-type (MYC) (Chico et al., 2020). The described transcription factors are involved in a wide range of processes including abiotic stress tolerance (Mooney et al., 2019; Morimoto et al., 2017), abscisic acid (ABA) and jasmonic acid (JA) signaling (Chico et al., 2020; Lechner et al., 2011), flowering time control (Chen et al., 2015), embryo development (Chen et al., 2015; Zhang et al., 2013), and fatty acid metabolism (Chen et al., 2013; Ma et al., 2015). In addition, protein phosphatases type 2Cs (PP2C), which are negative regulators of ABA signaling, are also recognized by BPMs (Julian et al., 2019). So far, BPM-substrate assembly always results in degradation of the targeted substrate protein.

Two motifs have been described in proteins that facilitate their recognition and binding by a BPM protein (Mooney et al., 2019; Morimoto et al., 2017; Zhuang et al., 2009). First, a Speckled-type POZ (SPOP)-Binding Consensus (SBC) motif, which comprises five amino acid residues of the order ϕ-π-S-S/T-S/T (ϕ, nonpolar; π, polar) (Zhuang et al., 2009). SPOP is the human BPM ortholog, and previous work demonstrated that the SBC motif is directly interacting with SPOP (Zhuang et al., 2009). Recent work in plants further showed that the motif is highly conserved among human and plants, and appears to be present in most, if not all, BPM substrates (Morimoto et al., 2017). Deletion of the SBC motif in the ERF/AP2 transcription factor Dehydration-responsive element-binding protein 2A (DREB2a) increased its stability without compromising its activity (Sakuma et al., 2006). Because DREB2a is a positive modulator of heat and drought stress responses, plants with increased DREB2a activity display improved tolerance toward these stressors (Morimoto et al., 2017; Sakuma et al., 2006). The second motif is a PEST motif that is enriched in the amino acids proline (P), glutamate (E), serine (S) and threonine (T), and is often associated with protein instability (Belizario et al., 2008; Mooney et al., 2019). Because it is less well defined, computational analysis is required to predict a probable PEST region (e.g. epestfind; http://emboss.bioinformatics.nl/cgi-bin/emboss/epestfind). However, it has been demonstrated that deletion of this motif significantly increases stability of the two ERF/AP2 transcription factors, Wrinkled1 (WRI1) and Related to Apetala2.4 (RAP2.4) (Ma et al., 2015; Mooney et al., 2019), and it is a critical requirement for normal assembly with BPMs (Mooney et al., 2019).

Here we show that overexpression of SBC or PEST motifs can be effective tools to modify stress tolerance and specific developmental features in Arabidopsis by affecting the ability of BPM proteins to bind to their substrates. This research can be used as a potential novel biotechnological tool to change agricultural traits in crop plants.

2 | RESULTS

2.1 | Generating unstable SBC- and PEST-motifs as tools to transiently interfere with BPM substrate binding

We recently showed that PEST motifs from *A. thaliana* and *Brassica rapa* RAP2.4 are sufficient for interaction with a BPM protein (Mooney et al., 2019), whereas Morimoto and co-workers demonstrated that highly conserved SBC- and SBC-like motifs also directly bind to BPMs (Morimoto et al., 2017).

We were interested in using these elements to design a system that would allow to transiently block BPM access to its substrates, and thereby prolonging substrate half-lives. However, the PEST motif from *B. rapa* BrRAP2.4-1 fused to GST (GST:PEST) is highly stable in cell-free degradation assays (Figure 1a), and we assumed that the SBC motif behaves similarly. Because constitutive down-regulation of all BPMs through artificial microRNA (*6xamiRNA*) broadly affects plant development (Chen et al., 2013), we expected that overexpression of stable SBC or PEST motifs would be similarly pleiotropic.

In order to design unstable SBC and PEST motifs that would only transiently block CRL3[BPM] activities, we decided to take advantage of the UBQ-fusion system (Bachmair et al., 1986). This system facilitates ubiquitin-proteasome dependent degradation of proteins via the N-degron pathway and uses PROTEOLYSIS 1 (PRT1) (Dong et al., 2017; Mot et al., 2018), an E3 ligase that works independently of CRL3[BPMs]. We utilized a system that was previously published by the Varshavsky group (Bachmair et al., 1986; Bachmair & Varshavsky, 1989), which has a UBQ fused to a 45 amino acid long lysine-containing extension (UBQ:eK). Any protein added C-terminally to the UBQ:eK becomes unstable *in planta* after the UBQ has been cleaved off post-translationally by endogenous de-ubiquitylation enzymes, which expose previously dormant N-degrons (Faden et al., 2014; Faden et al., 2016). In our case, the exposure of a phenylalanine (F) residue that is located N-terminally of the eK-element is anticipated to trigger recognition by PRT1, and subsequent degradation of the eK element and any attached additional peptides (Figure S2).

As shown in Figure 1b, recombinant GST-tagged UBQ:eK:SBC and: PEST proteins are highly unstable and are not detectable within 60 min in cell-free degradation assays. To verify that the UBQ:eK tag is not interfering with BPM interaction, pulldown assays were performed with GST:UBQ:eK:PEST and GST:UBQ:eK:SBC. Both were able to precipitate His:BPM1 and His:BPM3 (Figure 1c).

As a control, we generated a mutated version of the SBC motif in which all serine residues were changed to alanine (VTSTSS to VTATAA; GST:UBQ:eK:SBC[mut]). The changes in the mutant SBC
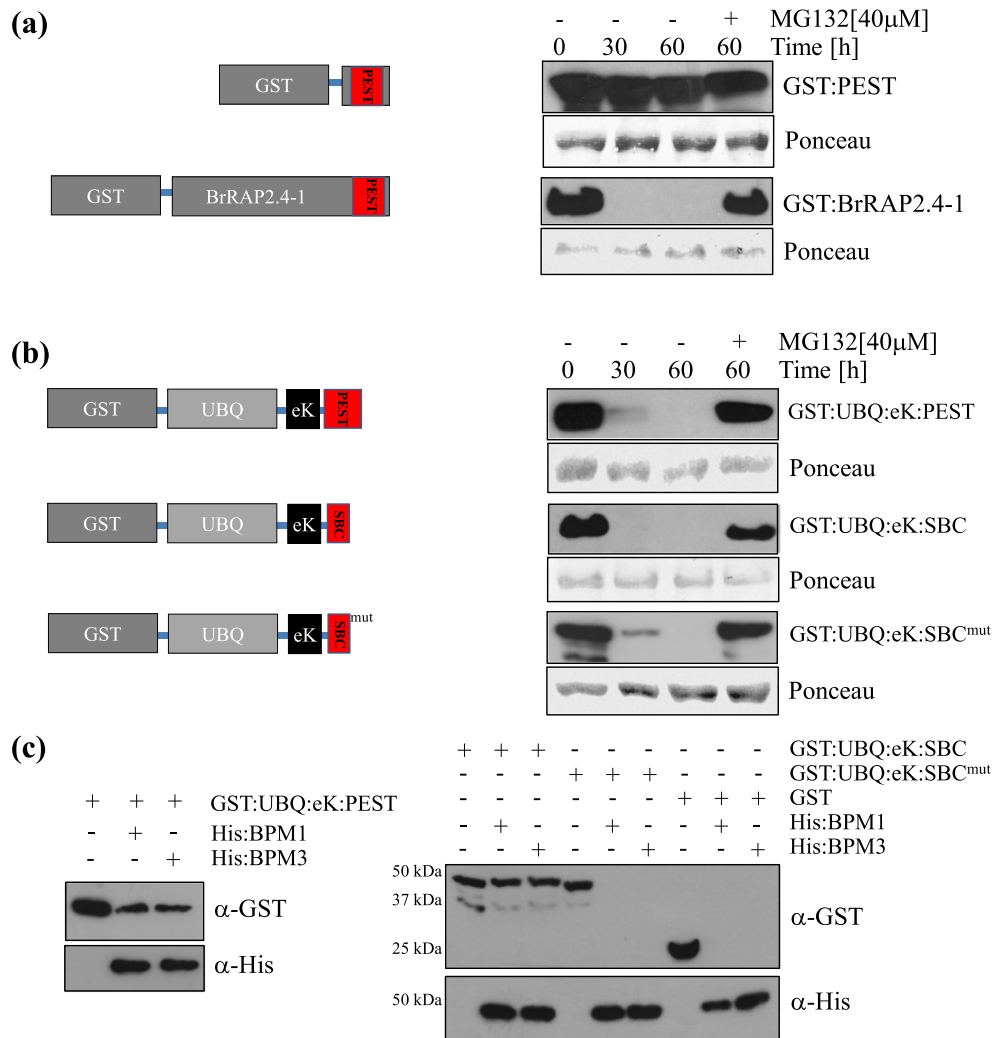
FIGURE 1 PEST and SBC motif stabilities and interactions with BPM proteins. (a) Left: Schematic drawing of BrRAP2.4-1 and its PEST motif, respectively. Right: In comparison with full-length GST:BrRAP2.4-1 the GST:PEST motif alone is stable as shown in cell free degradation assays. MG132, proteasomal inhibitor. (b) Left: Schematic drawing of different recombinant GST proteins fused to UBQ:eK:PEST, UBQ:eK:SBC, or UBQ:eK:SBC^{mut}. Right: Cell free degradation assays show that all three recombinant proteins are not detectable after 60 min. (c) Pulldown assays show interaction of the PEST (left) and SBC (right) GST-fusion proteins with His:BPM1 and: BPM3, whereas SBC^{mut} and GST alone did not interact. GST-tagged proteins were eluted, whereas His:BPMs remained on Ni-NTA beads. Sizes of detected proteins in alphabetical order: GST:BrRAP2.4-1, ~63 kDa; GST:PEST; ~35 kDa GST:UBQ:eK:SBC, ~42 kDa; GST:UBQ:eK:SBC^{mut}; ~42 kDa; GST:UBA:eK:PEST, ~47 kDa; His:BPM1, ~48 kDa; His:BPM3, ~46 kDa; GST, ~28 kDa. Sizes of different fusion protein domains in amino acids: BPM1: 422; BrRAP2.3: 322; GST: 240; His: 6; SBC and SBC^{mut}: 15; PEST: 62; UBQ:eK: 114. Loaded recombinant protein: His:BPM1 and 3, 250 ng; GST:UBQ:eK:PEST and: SBC, 50 ng; GST, 100 ng

disrupt interaction with a BPM protein (Figure 1c), but the GST:UBQ:eK:SBC^{mut} otherwise was degraded in a similar fashion as observed for the wild type SBC and PEST fusion proteins (Figure 1b). For simplicity, we named the two systems U-PEST and U-SBC.

2.2 | U-PEST and U-SBC can interfere with BPM-substrate interaction

To test whether U-PEST and U-SBC have the potential to affect BPM substrate binding *in planta* and thereby cause increased stability of

substrates, we performed competition experiments to see if the PEST and SBC motifs can bind to a BPM protein while reducing or even preventing BPM-substrate assembly. For these experiments increasing amounts of eluted recombinant GST-tagged U-PEST and U-SBC were pre-incubated with His:BPM1 before a BPM substrate was added. To investigate this, we used a verified substrate from *B. rapa*, BrRAP2.4-1, which shows the same interaction and functional properties as its Arabidopsis ortholog (Mooney et al., 2019).

As shown in Figure 2a,b, both U-PEST and U-SBC were able to block interaction between His:BPM1 and BrRAP2.4-1. Of note is that for disruption of BPM-substrate interaction, 500 ng U-PEST was
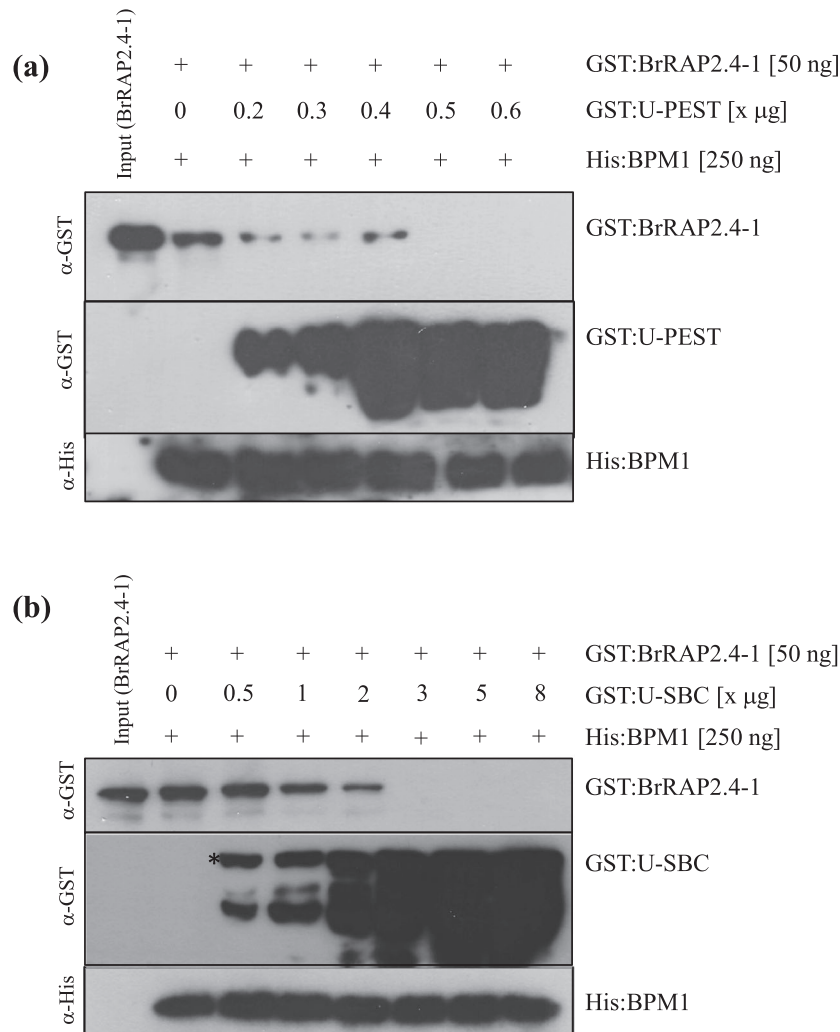
(a)

FIGURE 2 SBC and PEST motifs can compete with BrRAP2.4-1 for binding to a BPM protein. (a) Competition pulldowns using a recombinant GST:U-PEST show that 500 ng are necessary to block binding of BrRAP2.4-1 to His-tagged BPM1. (b) The same assay done with recombinant GST:U-SBC protein shows that 3000 ng are required to block BrRAP2.4-1/His:BPM1 binding.

(b)

sufficient under the tested conditions, whereas we had to use around 3000 ng of U-SBC to get the same result. This is consistent with previous results where we observed stronger impacts on BPM-substrate assembly when the PEST motif was deleted in comparison to proteins lacking the SBC motif (Mooney et al., 2019). The high amounts of U-SBC necessary to block BPM-BrRAP2.4-1 assembly indicates that the affinity or binding of U-SBC to a BPM protein is likely comparably low or unstable, respectively.

2.3 | U-PEST and U-SBC increase BPM substrate stability in cell-free degradation assays

To investigate whether U-PEST and U-SBC can affect substrate stability, we took advantage of a cell-free degradation assay (Mooney et al., 2019). Here we used U-PEST (500 ng) and U-SBC (3000 ng) amounts that were established in the pulldown assays as being able to disrupt BPM-substrate interaction. As substrates we used two different proteins from *B. rapa*, BrRAP2.4-1 and BrWRI1.2, and one Arabidopsis protein, AtMYB56. Both BrRAP2.4-1 and BrWRI1.2 are members of the ERF/AP2 family and closely related to the
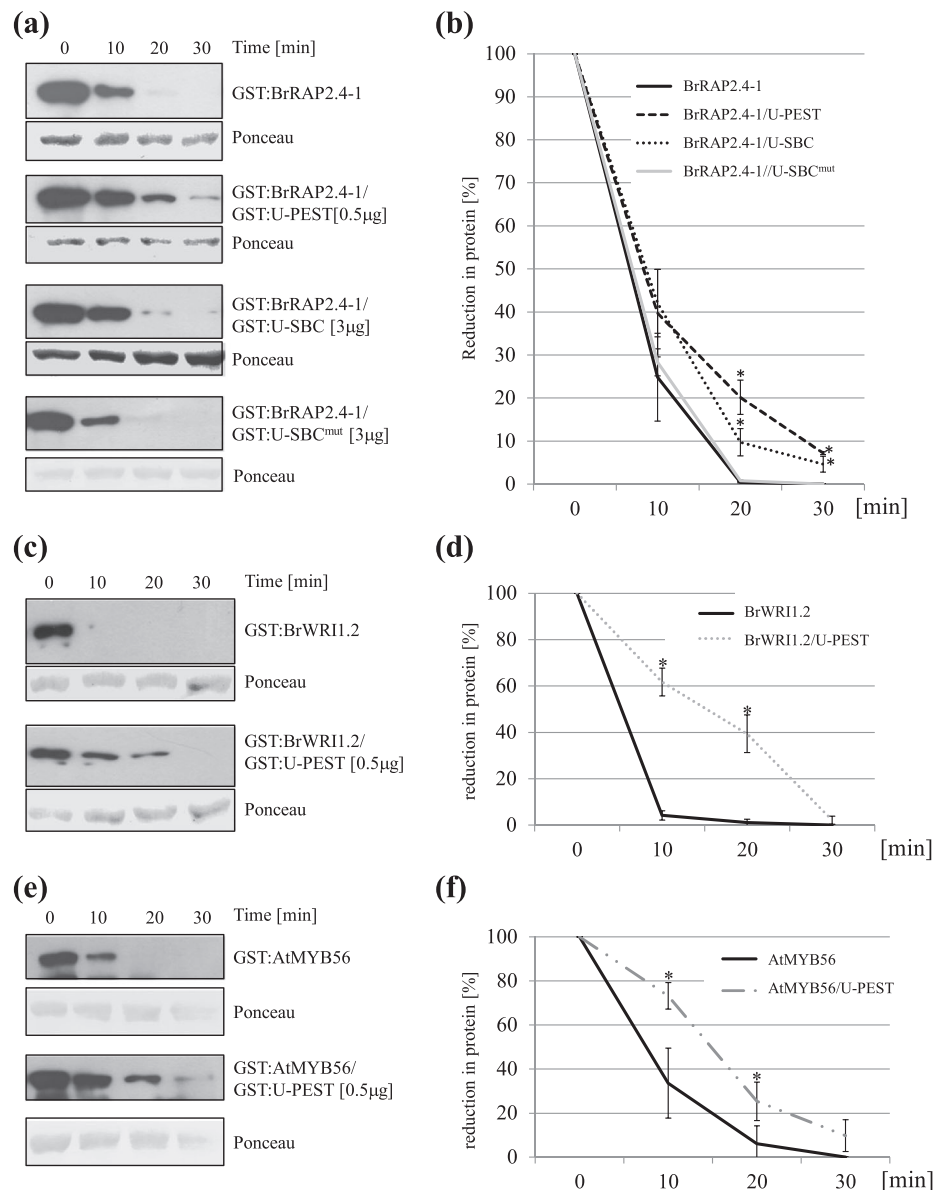
Arabidopsis orthologs, AtRAP2.4 and AtWRI1, for which we had previously demonstrated their function as BPM substrates (Chen et al., 2013; Mooney et al., 2019). AtMYB56 is a member of the MYB transcription factor family, and is also a proven BPM interactor (Chen et al., 2015).

We first tested recombinant GST:BrRAP2.4-1 protein and observed that the addition of either U-PEST or U-SBC significantly delayed degradation of the BPM substrate (Figure 3a,b). However, U-SBC was clearly less effective than U-PEST. We also tested UBQ:eK:SBC^mut (3000 ng) as a control and did not see any significant changes in BrRAP2.4-1 stability (Figure 3a,b).

This further corroborates that the delayed BrRAP2.4-1 degradation requires functional U-PEST and U-SBC to block BPM proteins. In addition, it shows that the delay in BrRAP2.4-1 degradation is not caused by the additional protein added to the cell-free degradation assay.

To significantly increase BrRAP2.4-1 stability very high amounts of the U-SBC motif were required, indicating that the SBC motif was comparably ineffective in blocking BPM activities. For this reason, in the following cell free degradation assays, we decided to focus on U-PEST. As shown in Figure 3c–f, both BrWRI1.2 and AtMYB56 became

FIGURE 3 Cell-free degradation assays show increased stability of BPM substrates in the presence of SBC or PEST motifs. (a) Cell-free degradation assays show that BrRAP2.4-1 degradation is delayed when either U-PEST or U-SBC are present in the assay, whereas GST:U-SBC^mut has no impact on how quickly BrRAP2.4-1 is degraded. (b) Quantification of results shown in (a). Similar results are seen for BrWRI1.2 (c, d) and AtMYB56 (e, f). Quantifications are based on at least three biological replicates. In this and all subsequent figures: *$p < .05$ and **$p < .01$. Error bars show standard deviation.

(a)

Time [min]				
0	10	20	30	

GST:BrRAP2.4-1
Ponceau

GST:BrRAP2.4-1/ GST:U-PEST[0.5μg]
Ponceau

GST:BrRAP2.4-1/ GST:U-SBC [3μg]
Ponceau

GST:BrRAP2.4-1/ GST:U-SBC^mut [3μg]
Ponceau

(b)

(c)

Time [min]				
0	10	20	30	

GST:BrWRI1.2
Ponceau

GST:BrWRI1.2/ GST:U-PEST [0.5μg]
Ponceau

(d)

(e)

Time [min]				
0	10	20	30	

GST:AtMYB56
Ponceau

GST:AtMYB56/ GST:U-PEST [0.5μg]
Ponceau

(f)

notably more stable in the presence of U-PEST. These results show that by adding a U-PEST or U-SBC protein to these cell-free degradation assays, we can increase half-life of known CRL3^BPM E3 ligase substrates. It further shows that this system is not limited to a specific type of transcription factor and likely not restricted to proteins from a specific plant species.

2.4 | Generation of transgenic plants expressing U-PEST and U-SBC

Many of the described BPM targets are involved in abiotic stress tolerance and ABA signaling (Julian et al., 2019; Lechner et al., 2011; Mooney et al., 2019; Morimoto et al., 2017; Weber & Hellmann, 2009). We hypothesized that under the control of a stress and ABA inducible promoter, expression of U-PEST and U-SBC may

have detectable impacts on plant stress responses by transiently increasing half-life of BPM substrates (see Figure S2). Because constitutive reduction in *BPM* expression affected plant development (Chen et al., 2013; Chen et al., 2015; Lechner et al., 2011), we also generated *U-PEST* and *U-SBC* expression constructs under the control of a *35S* promoter to see if this had the same impact. Several transgenic plant lines were generated expressing U-PEST and U-SBC, either under the control of a *proRD29A* (inducible by drought, salt, cold, and ABA) or a constitutively active *pro35S* promoter. At least 40 independent plants per construct were found, and two independent lines were chosen that showed clear constitutive (*pro35S*) (Figure 4a) or salt-inducible (*proRD29A*) (Figure 4b) U-PEST and U-SBC expression, respectively. Despite the detection of high expression levels for *U-PEST* and *U-SBC*, we were only able to detect a GFP protein in the transgenic plants in Western-blots. The protein ran at 35 kDa, which matches the expected size of GFP:UBQ.
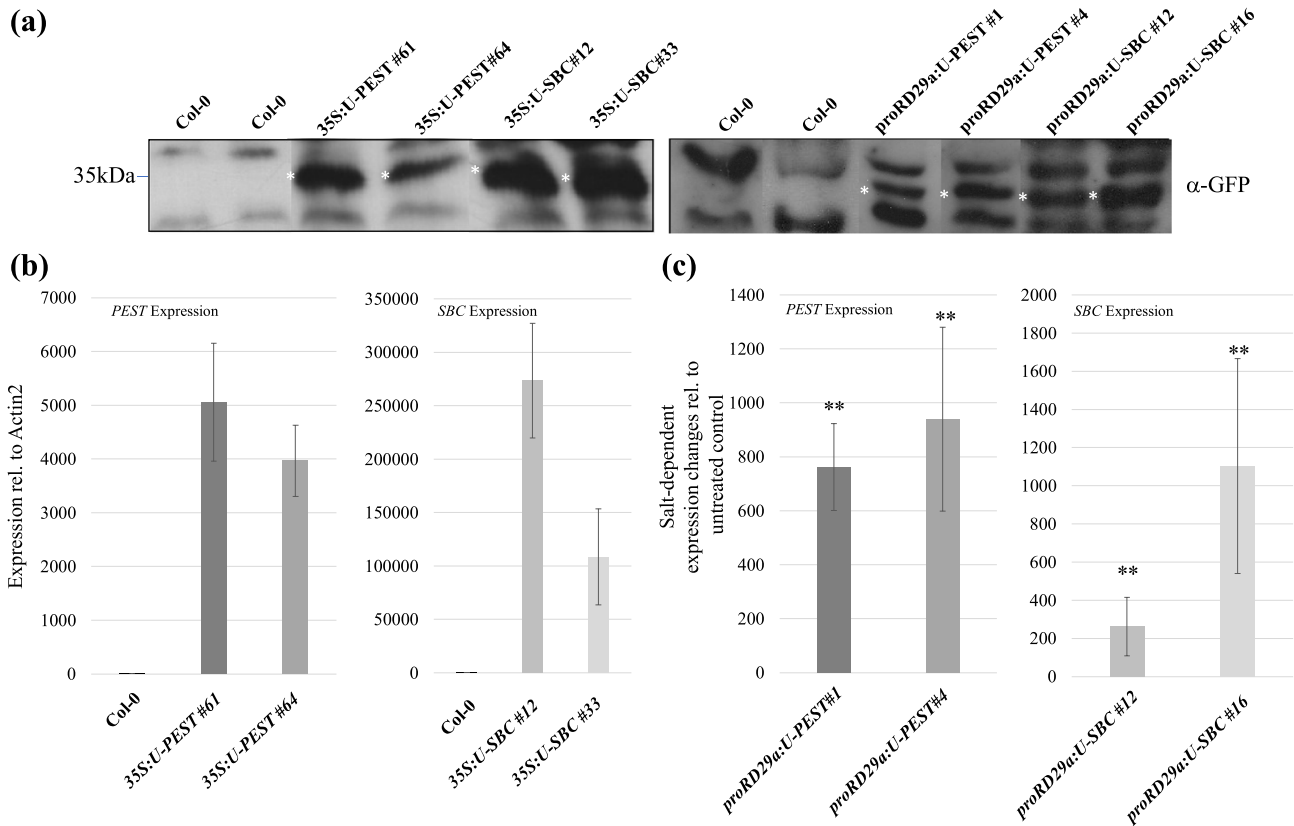
(a)

(b)

(c)

FIGURE 4 Expression analysis in *pro35S: And proRD29:U-PEST* and *U-SBC* plants. (a) Western-blot analysis testing GFP expression in either *pro35S:U-PEST and: U-SBC* (left) or *proRD29a:U-PEST or: U-SBC* (right; salt treated; 300 mm for 5 h) plant lines. Asterisks indicate presumed band for GFP:UBQ (~35 kDa); 200 μg total protein extract were loaded per lane. (b) RT-qPCR analysis of *U-PEST* (left graph) and *U-SBC* expression (right graph) in two independent *pro35S* transgenic lines, respectively. No expression was detectable in Col-0 wildtype controls. **Significant difference in expression ($p < .01$) compared with Col-0. (c) RT-qPCR analysis of salt inducibility of *U-PEST* and *U-SBC* under the control of a *RD29a* promoter. Shown is the fold change compared with untreated controls. Plants were treated for 5 h with 300 mM NaCl before samples were harvested. **Significant upregulation ($p < .01$) compared with untreated plants. Data in (a) and (b) are based on $n = 4$ biological replicates.

2.5 | U-PEST and U-SBC expression affect stress tolerance and development

The *RD29a* promoter is inducible by salt, cold, drought and osmotic stress, as well as ABA treatment (Arabidopsis eFP browser at bar.utoronto.ca). Consequently, transgenic *proRD29A:U-PEST* and :*U-SBC* plants were tested for their sensitivity at the germination and seedling stages when exposed to these different growth conditions (Figure 5a). In general, transgenic seeds germinated to the same degree and within the same time frame as wild type seeds (Figure 5b). With respect to ABA and mannitol, we also did not observe that the transgenic seeds germinated significantly different to the wild type Col-0 (Figure S3). However, when exposed to salt stress the transgenic seeds germinated significantly faster than wild type seeds (Figure 5c,d), and this was more pronounced for the U-PEST expressing plants, which at days two and three after plating on 150 mM NaCl showed a 30%–40% higher germination rate than the wild type (Figure 5c). U-SBC plants displayed only a mildly faster germination rate compared with wild type and only at 100 mM NaCl (Figure 5d). This slight advantage was gone when seeds were plated on 150 mM

NaCl (Figure S4). In the cold (4°C) both U-PEST and U-SBC germinated slightly but significantly faster than wild type seeds (Figure 5e).

For root elongation assays we observed shorter roots specifically for the U-PEST seedlings compared with wildtype plants (Figure 5f). In addition, both U-PEST and U-SBC plants showed less inhibition of primary root growth when exposed to NaCl compared with unstressed conditions (Figure 5g,h). Consistent with the germination data, U-PEST plants appeared to be more tolerant than U-SBC plants because higher salt concentrations could be applied to U-PEST seedlings (125 mM NaCl vs. 100 mM for U-SBC) with significant differences to wild type seedlings still observed (Figure 5g,h). Plants expressing either U-PEST or U-SBC also behaved more insensitive to ABA (20 μM) in the root elongation assays (Figure 5i). This was surprising because no altered sensitivity was detected in the germination assays (Figure S3).

We further tested how constitutive expression of *U-PEST* and *U-SBC* affect stress tolerance at the germination and seedling stage (Figure 6a). Transgenic seeds did not behave differently compared with wild type under normal growth media (Figure 6b). Like for *proRD29a:U-PEST* and :*U-SBC* plants, we did not observe any differences
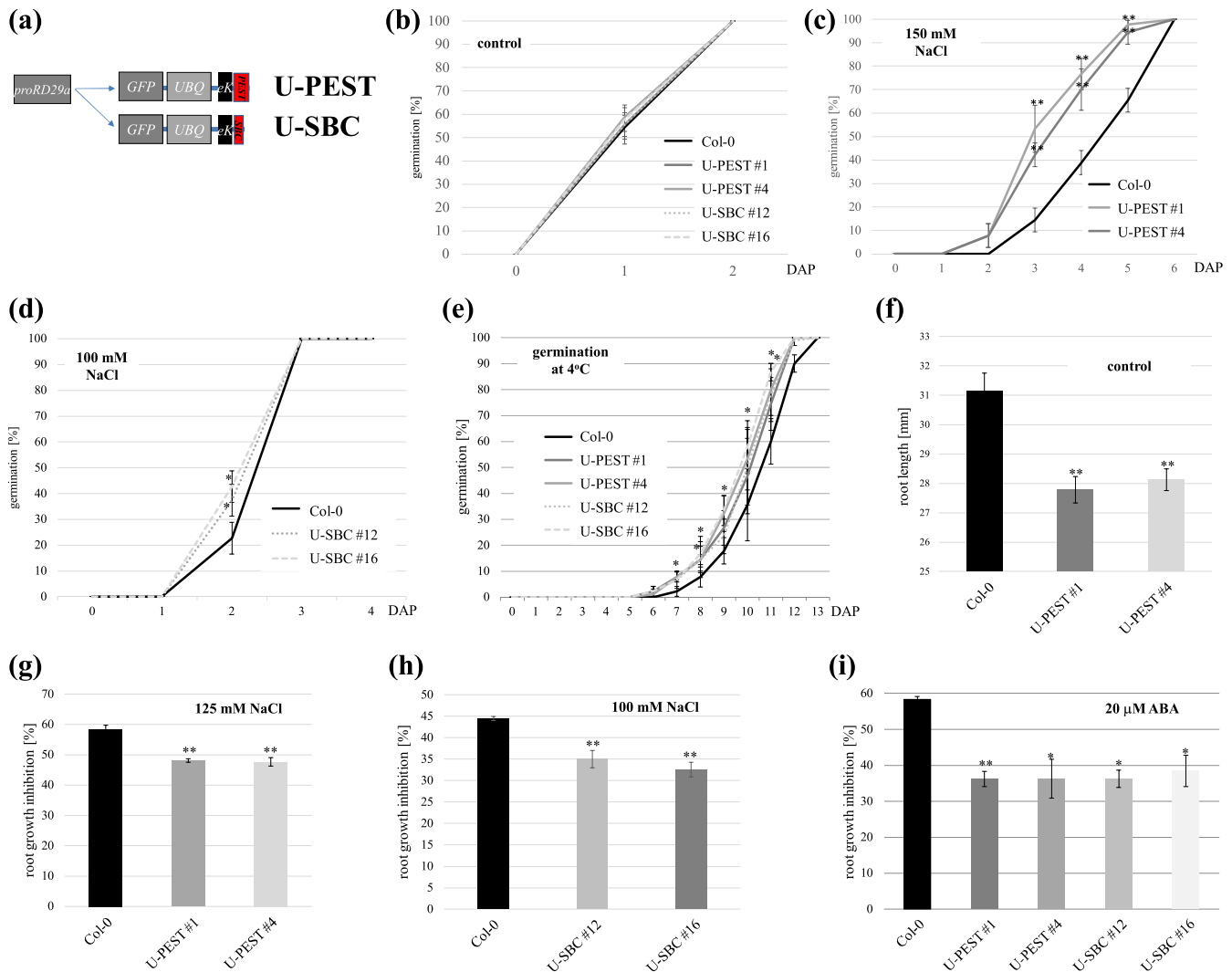
FIGURE 5 Impacts of *U-PEST* and *-SBC* under the control of an *RD29A* promoter. (a) Schematic drawing of the *proRD29A:U-PEST* and *-SBC* constructs introduced into Arabidopsis. Germination assays (b to e) show no difference between transgenic seeds and wild type under normal growth conditions (b), whereas for salt, both *U-PEST* (c) and *-SBC* (d) germinated earlier than wild type. Also, under cold conditions both *U-PEST* and *-SBC* germinated faster compared with wild type seeds. (f) Root length of 10-days old *U-PEST* seedlings is significantly shorter than in wild type plants. All germination data in this graph are based on three biological replicates with $n = 30$ seeds per replicate. Root elongation assays (g to i) show that elongation growth is significantly less inhibited in transgenic plants by salt (g, *U-PEST*; h, *U-SBC*) and ABA (i) compared with wild type. Inhibition was calculated as reduced length in the presence of NaCl or ABA, respectively, to root length under non-stressed conditions. Root elongation data in this figure are based on three biological replicates, and at least $n = 20$ individual plants per replicate. DAP, days after planting. *$p < .05$; **$p < .01$

in germination on ABA and mannitol containing plates (Figure S3A, B), but faster germination was detected under cold conditions (Figure 6c), and on plates supplemented with NaCl (Figure 6d). For ABA and salt-dependent root elongation assays, we again observed reduced elongation growth in the transgenic seedlings relative to untreated conditions (Figure 6e–g). We also included JA because CRL3^{BPM} E3 ligases have been recently described to be involved in the response regulation of this phytohormone (Chico et al., 2020). Because the *RD29a* promoter is not inducible by this phytohormone, whereas the *35S* promoter results in constitutive expression of the respective transgene, we only tested this phytohormone on the *pro35S:U-PEST/-SBC* plants. Like for ABA and salt, we also observed

a mild tolerance of *U-PEST* and *U-SBC* expressing plants to JA exposure (Figure 6h).

To test whether stress tolerance is also observable at later stages in development, we focused on salt tolerance, as this gave robust phenotypes at the germination and seedling stages. Three-week old plants were watered for 3 weeks with a 200 mM NaCl solution every 3 days. After the 3 weeks, living plants in comparison to dead plants, (for reference see Figure S3C) were counted. We observed a significantly higher number of survival rates for *pro35S:* and *proRD29A:U-PEST*, which in average was around 30%–40% higher compared with wild type (Figure 7), further corroborating that salt sensitivity can be significantly reduced by expressing the PEST motif. We included the
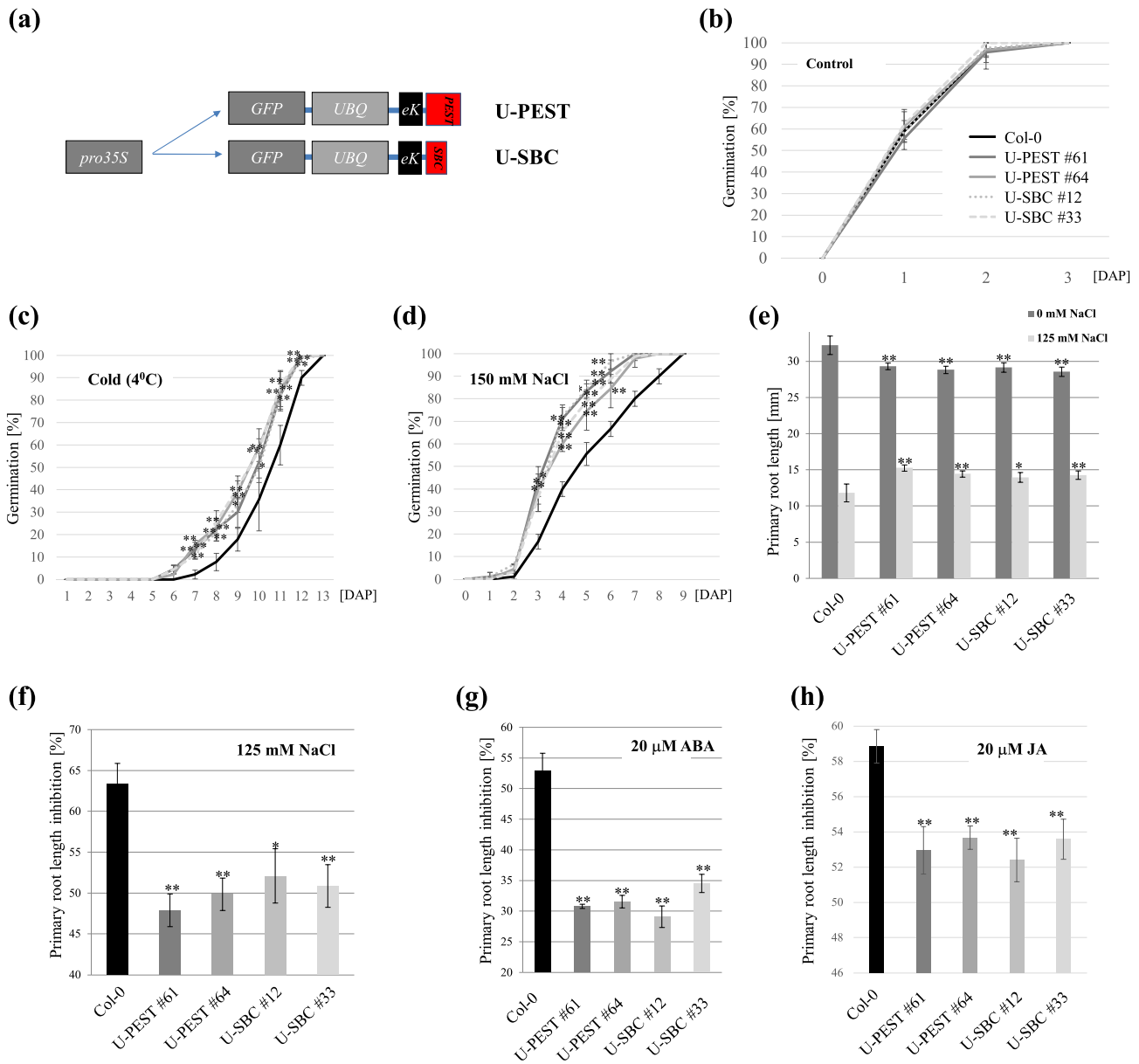
FIGURE 6 Early impacts of *U-PEST* and *U-SBC* under the control of a *35S* promoter. (a) Schematic drawing of the *U-PEST* and *-SBC* constructs introduced into Arabidopsis. Germination assays (b to d) show no difference between transgenic seeds and wild type under normal growth conditions (b), whereas for cold (c) and salt (d), both *U-PEST* and *-SBC* seeds germinated earlier than wild type. All germination data in this graph are based on three biological replicates with $n = 30$ seeds per replicate. (e) Root lengths of 10 days old U-PEST and -SBC seedlings are significantly shorter than in wild type plants. Root elongation assays (f to h) show that elongation growth is significantly less inhibited in transgenic plants by salt (f), ABA (g), and JA (h) compared with wild type. Root elongation data in this figure are based on three biological replicates, and at least $n = 20$ individual plants per replicate

U-SBC lines in our first trials, but did not observe clear differences in soil salt sensitivities compared with Col-0 (Figure S3D), and therefore did not further investigate these lines.

Overall plants expressing *U-PEST* and *U-SBC* under the control of the *35S* promoter were not significantly affected in development. In addition to a shorter root at the seedling stage (Figure 6e), we only observed a delayed flowering time (Figure 7c), also observed in plants with reduced BPM expression levels (Chen et al., 2015). There were no differences in seed yield per silique, although a small, but

significant, increase in average seed weight for the two U-PEST lines (11 and 7%, respectively) compared with wild type was measured (Figures S3D and 7d).

3 | DISCUSSION

The current work demonstrated that expression of either an SBC or a PEST motif alone is sufficient to block binding of BPM proteins to
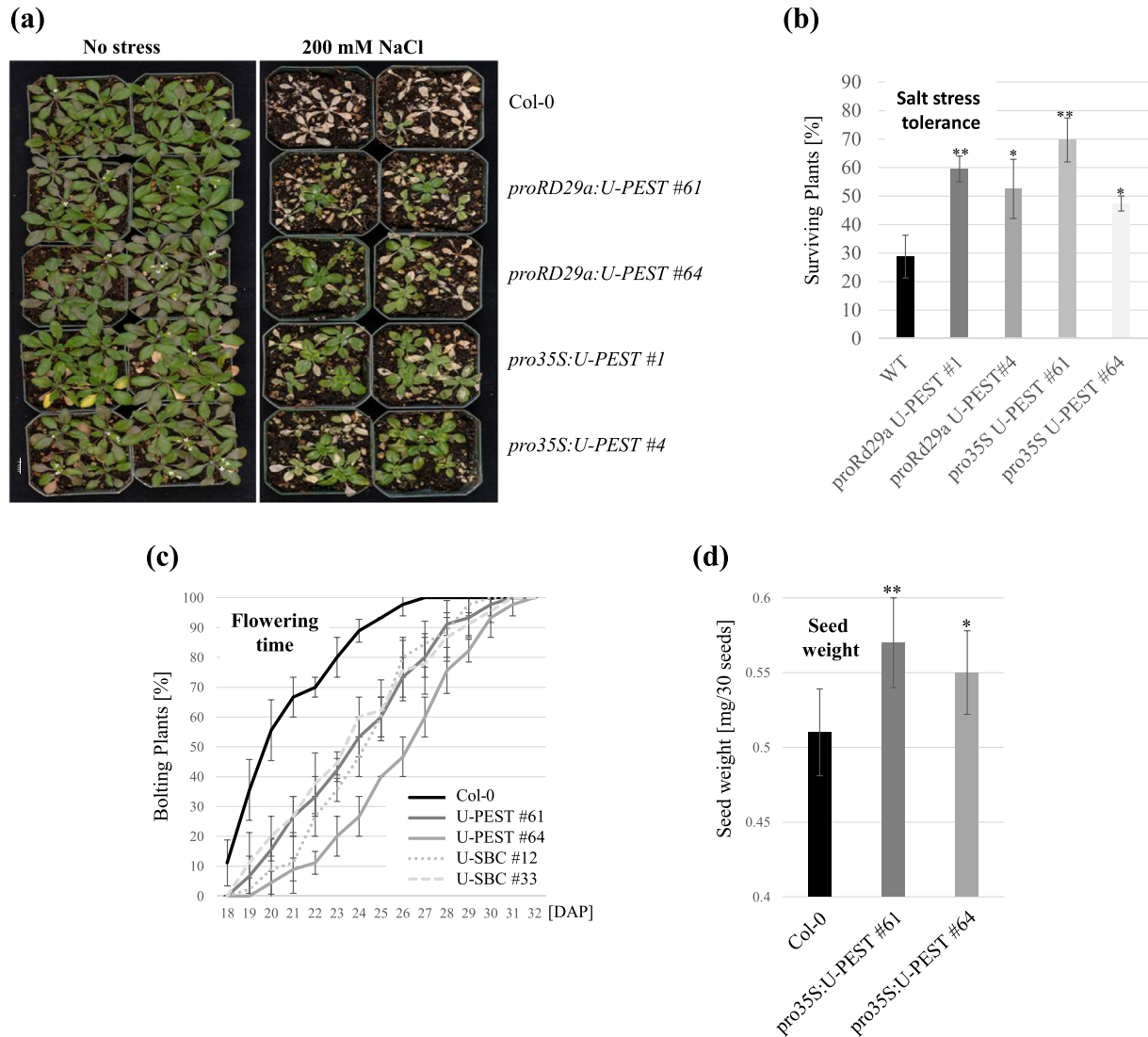
(a)

(b)

(c)

(d)

FIGURE 7 Later impacts of *U-PEST* and *U-SBC* under the control of *35S* and *RD29A* promoters. (a) The growth of transgenic Arabidopsis under normal conditions and salt stress (200 mM NaCl) compared with wild type. (b) Soil salt stress treatments (200 mM NaCl) show significantly higher survival rates of *pro35S:* And *proRD29A:U-PEST* plants compared with wild type. Data are based on three biological replicates with $n = 100–120$ plants per genetic background tested in each biological replicate. (c) *pro35S:U-PEST* and *-SBC* flowering time is significantly delayed compared with wild type. All data between days 21 and 27 show significant differences between transgenic and wild type plants of at least $p < .01$. Days 19, 20, and 31 values are at least $p < .05$. Data are based on three biological replicates with $n = 15$ plants per replicate. (d) *pro35S U-PEST* lines have slightly but significantly heavier seeds compared with wild type. Data are based on five biological replicates.

their substrates. This can result in increased BPM substrate stabilities, and thereby affect plant stress tolerance and development.

The phenotypes observed are overall consistent, and in agreement, with previously described changes caused by altering *BPM* expression levels and, consequently, increased stability and activity of BPM substrates. For example, Arabidopsis plants affected in all six BPMs through expression of an *amiRNA* (*6xamiBPM*) also have shorter roots and a delayed flowering phenotype, as well as heavier seeds, specifically in the two *35S:U-PEST* lines (Chen et al., 2013, 2015). The shorter root is likely caused in part by stabilization of the BPM substrate MYB56/BRAVO, which has been reported to reduce root apical meristem activity (Chen et al., 2015; Vilarrasa-Blasi

et al., 2014). The delayed flowering time of *6xamiBPM* plants was brought in context with a delayed expression of *FLOWERING LOCUS T* (*FT*), a promoter and master regulator of flowering time in Arabidopsis (Chen et al., 2015; Song et al., 2013). We also observed changes in seed weight for the two 35S:U-PEST lines, which is likely contributed to by increased WRI1 activities, but may also relate to elevated MYB56 protein levels (Chen et al., 2013; Zhang et al., 2013). The comparably mild changes in seed size compared with the *6xamiRNA* approach might be due to the short half-lives of the U-PEST/U-SBC proteins, and one may observe different results if their half-lives would be either longer, or if the U-PEST/U-SBC constructs would be expressed under a more specific promoter, such as *WRI1* that serves

as the master regulator of seed oil production in Arabidopsis (Chen et al., 2013; Focks & Benning, 1998).

Although connections to the ABA signaling pathway have been made a couple of times, no reports so far show that reduced BPM activity affects ABA-dependent seed germination (Julian et al., 2019; Lechner et al., 2011). However, overexpression of MYB25, a novel, recently described BPM substrate, confers reduced ABA sensitivities at the germination stage (Beathard et al., 2021), whereas overexpression of *BPM3* or *BPM5* was demonstrated to increase ABA-dependent root elongation sensitivity in seedlings (Julian et al., 2019). Consistent with that, we observe reduced ABA sensitivity in this work. In addition, reduced *BPM* expression also negatively affects stomata closure in response to drought stress, likely by stabilizing PP2C and AtHB6, which are both negative ABA response regulators (Julian et al., 2019; Lechner et al., 2011). Although we did not investigate this specific phenotype in our U-PEST and U-SBC plants, one can anticipate that they may also be affected in stomatal closure control.

A couple of confirmed BPM targets support the changed seed germination rate under cold temperature condition. Papaya RAP2.4 improves cold tolerance when overexpressed in tobacco (Figueroa-Yanez et al., 2016), and enhanced expression of the BPM substrate DREB2a confers freezing tolerance in Arabidopsis (Sakuma et al., 2006). In addition, the BPM interacting protein DREB1a also acts as a positive cold-stress response regulator (Donde et al., 2019; Maruyama et al., 2004); though interplay of this protein with BPMs has only been shown through yeast-2-hybrid assays (Chen et al., 2013). However, for all these proteins, it is likely that they are more stable when BPMs are blocked by U-PEST or U-SBC, which supports the faster germination rate at 4°C.

Arabidopsis MYB25 and RAP2.4, from either Arabidopsis or *B. rapa*, are also known to improve salt tolerance in plants (Beathard et al., 2021; Mooney et al., 2019; Phuong & Hoi, 2015), which would be in agreement with findings in this work that seeds germinated faster on NaCl containing plates and seedlings had reduced sensitivity in root elongation assays.

Finally, the reduced JA sensitivity of our U-PEST and U-SBC plants was surprising because a recent report showed that plants negatively affected in BPM activity have increased stability of MYC2 and MYC3, two transcription factors that act as positive response regulators of this phytohormone (Chico et al., 2020). These studies further showed reduced root length under normal growth conditions in *amiR-bpm* plants that are affected in BPM1, 4, 5, and 6 (Chico et al., 2020; Lechner et al., 2011). Although the shorter root is consistent with our findings, the *amiR-bpm* plants have also significantly shorter roots compared with wild type after exposure to JA (Chico et al., 2020), whereas we observed no significant difference in root length between the wild type and the transgenic U-PEST and U-SBC plants under these conditions (Figure S5). This leads to different interpretations of JA sensitivity in our research compared with previous studies (Chico et al., 2020). The reason for this difference is unclear at this point, but may either be related to the different approaches, or that we impact all six BPMs in the U-PEST/U-SBC expressing plants, and not just four, like in *amiR-bpm* seedlings.

The employment of the UBQ-fusion system is anticipated to allow for controlled instability of the two motifs in the cell and to facilitate, in combination with the eK element, that the SBC and PEST moieties are quickly depleted from the cell. However, we cannot fully exclude at this time that the degradation of eK:PEST and eK:SBC is also triggered by interaction with BPMs, as these proteins function as substrate adaptors of a CRL3^{BPM} E3 ligase. Regardless, the overall outcome of protecting BPM substrates from degradation will be the same.

As mentioned above, the UBQ-fusion system depends on the activity of de-ubiquitylation enzymes that co-translationally cleave off the UBQ (Varshavsky et al., 1989) and appear to remain active in cell-free degradation assays. The resulting C-terminal fragment then becomes a target of the plant's N-degron pathway (Dissmeyer, 2019). The N-terminal UBQ-containing fragment itself can become a target of the UBQ fusion degradation pathway (UFD) (Johnson et al., 1992). Critical for the half-life of the adjacent fragment is its N-terminal amino acid residue, which in our case is phenylalanine (see also Figures S1 and S2) and results in a comparably quick degradation (Dissmeyer, 2017; Faden et al., 2019). In order to increase half-lives of the U-PEST or U-SBC in the cell, one could replace the Phe with an amino acid that confers longer stability, such as alanine or isoleucine, thereby enhancing the impact on cellular processes. In combination with specific promoters, this may serve in future applications as a powerful tool to affect specific plant traits that CRL3^{BPM} E3 ligases regulate.

This novel approach provides several advantages in comparison to alternative, previously published approaches that modulate CRL3^{BPM} activities or BPM substrate stabilities. This work demonstrates a proof-of-concept approach that CRL3^{BPM} activities can be specifically modulated to e.g., increase salt stress tolerance without impacting other developmental aspects. Alternative approaches such as amiRNA appear to be more aggressive, as seen by strongly delayed development (Chen et al., 2013, 2015; Lechner et al., 2011), a feature we did not observe in plants constitutively overexpressing U-SBC or U-PEST. In addition, one can expect that in most plant species several amiRNAs are needed to down-regulate most or all BPMs. Our approach, at least on what we observe so far for PEST/MATH domain interactions in Arabidopsis, is likely effective against most, if not all, BPMs in a given plant species. In addition, *in planta* half-life for amiRNA remains unclear, but reports from animal systems describe that their half-life ranges from minutes to hours, and even weeks (Krol et al., 2010; Reichholf et al., 2019; Rissland et al., 2011; van Rooij et al., 2007). Such negative regulators may impact plant processes over significant periods of time, and long after a specific promoter had been activated. In addition, microRNAs have been reported to move from cell to cell and may therefore impact a broader range of cells (Carlsbecker et al., 2010; Chitwood et al., 2009), which is likely not the case for our synthetic proteins due to rapid degradation. In fact, even weak expression of amiRNAs may have substantial impacts on targets based on subsequent actions of e.g. ARGONAUTE and DICER proteins (Paturi & Deshmukh, 2021; Wu et al., 2020). Another alternative approach could be to overexpress BPM substrates

that are modified to have reduced interaction with BPMs. However, this requires detailed information on BPM/substrate interactions so as not to compromise the substrate activity. Additionally, such an approach can only focus on one substrate at a time, and may not contribute much to our overall understanding about system wide impacts that depend on CRL3[BPM] activities. As a quintessence, this novel tool may be very suitable for system-wide level analysis on how CRL3[BPM]s affect processes specifically under stress, or in a specific organ or developmental stage. Pursuing this level of information may allow for novel insights into how this E3 ligase is interwoven with the cellular regulatory network, and to dissect its biological roles in diverse processes. It may also determine best individual candidate proteins for alternative, subsequent targeted approaches to improve relevant agricultural traits in plants. Because this E3 ligase is so highly conserved among plants, and other eukaryotes, one can anticipate that this approach may be useful for a broader range of crop plants, as well as research on animal organisms to investigate CRL3[BPM] activities.

4 | EXPERIMENTAL PROCEDURES

4.1 | Plant growth, transformation, and phenotypic analysis

A. thaliana plants Columbia-0 (Col-0) ecotype were grown under long-day (16 h light: 8 h dark) and standard growth conditions in soil and sterile culture as described before (Bernhardt et al., 2006). Plant transformations were done using the floral dip method (Clough & Bent, 1998). For germination assays only seeds from plants grown at the same time and under the same conditions were used. For germination and root elongation assays, basic culture medium was supplemented with either a phytohormone (abscisic acid or jasmonic acid) or salt (NaCl). Cold germination assays were done with seeds being consistently exposed to 4°C after plating. Germination was defined as the time point when the radicle first emerges from the seed coat. For root elongation assays seedlings were first grown vertically for 5 days on non-selective medium before being transferred individually to selective conditions. After five additional days root length was measured. Time of bolting was measured under long-day conditions. First signs of inflorescence development were defined as the day bolting started. Quantification of root length was done using ImageJ software (Schneider et al., 2012).

4.2 | Generation of expression constructs

The DREB2A SBC and mutant SBC motifs were synthesized and extended using specific primers, whereas *BrRAP2.4-1* (*Bra003659*) PEST motif was directly amplified from the corresponding cDNA (all primers used in this work are listed in Table S1). The corresponding products were generated with overhangs to allow PCR-based fusion to a *UBQ:eK* fragment (Naumann et al., 2016). *BrRAP2.4-1* and

AtMYB56 (*At5g17800*) genes were cloned as described earlier (Chen et al., 2015; Mooney et al., 2019). *BrWRI1.2* (*Bra003178*) was amplified from cDNA generated from *B. rapa* R-0-18 silique total RNA using an Isolate RNA Minikit (Bioline, NJ). cDNA was synthesized using a high-capacity DNA reverse transcription kit (Applied Biosystems, CA). For expression in *E. coli*, products were further amplified to add *NcoI/EcoRI* restriction sites for cloning into the *pHB2-GST* vector. For *His:BPM1* and: *BPM3* expression constructs both genes were shuffled from *pDONR221* into the vector *pDEST17* via Gateway LR reactions (Thermo Fisher Scientific, MA). For *in planta* expression, the different *UBQ:eK* fusion constructs were first cloned via Gateway BP reactions into *pDONR* [Zeocin] before they were shuffled into the binary vector *pMDC43* (Curtis & Grossniklaus, 2003). Constructs were generated using either the original *35S* promoter of *pMDC43* or an Arabidopsis *RD29a* promoter (Bihmidine et al., 2013) that was cloned via *HindIII/XbaI* restriction sites into *pMDC43* replacing the *35S* promoter. The *UBQ:eK:SBC*,: *SBC* [mut], and: *PEST* constructs were cloned 3′ of *pMDC43's GFP* gene. All constructs were verified before usage by sequencing for correct translational frame and absence of PCR-generated mutations. An overview of the amino acid sequences for UBQ:eK:PEST and: SBC is provided in Figure S6.

4.3 | Pulldown assays

For pulldown assays, purified recombinant proteins were expressed in *E. coli*, extracted and purified on either glutathione, for GST-, or Ni-NTA, for His- then quantified using silver-stained SDS-PAGE gels on which bovine serum albumin (BSA) proteins of known quantities were co-loaded as standard. Pulldown assays were done as described before (Chen et al., 2013) where His- proteins remained on the beads and were used to detect the interaction with eluted GST- proteins. For competition experiments, eluted GST:UBQ:eK:SBC,: SBC[mut], and: PEST were pre-incubated (30 min, 4°C) with His-tagged BPM proteins on Ni-NTA beads, before eluted GST:BrRAP2.4-1, BrWRI1.2, and AtMYB56 proteins were added.

4.4 | Western blot analysis

Proteins were separated on a 12% SDS-PAGE using a Hoefer SE260 Mighty Small II Mini Vertical Electrophoresis System (Hoefer, Holliston, MA) and blotted on a PVDF membrane (ThermoFisher, Waltham, MA, Cat. No. 88518) using a Bio-Rad Trans-Blot Turbo transfer system 690BR (BioRad, Hercules, CA, Cat. No. 1704150). Proteins were detected either with monoclonal GST (Cat. No. LT0423; Life Tein, NJ), monoclonal His (Cat. No. LT0426 LifeTein, NJ), polyclonal GFP (Cat. No. 10087-514; VWR International, Radnor, PA) antibodies or horseradish-coupled secondary goat anti-mouse and anti-rabbit antibodies from Santa Cruz, CA (Cat. No. sc-2005 and Cat. No. sc-2004, respectively). Antibody/protein interactions were visualized using standard chemiluminescent western blot detection (Cat. No. 34579; ThermoFisher, Waltham, MA) and Fuji medical X-ray film

(Cat. No. 47410 19291; Z&Z Medical Inc, Cedar Falls, IA). Films were developed and fixed using standard solutions.

4.5 | Cell-free degradation assays

The assays were done as described earlier (Mooney et al., 2019). In brief, for cell-free degradation assays, plant extracts (20 μg/time point) from 2-week-old sterile grown Arabidopsis seedlings were combined with purified, recombinant, and eluted GST proteins (100 μg/time point) and incubated for defined time periods at room temperature; 20 μl samples were taken at indicated time points and used for SDS-PAGE and Western-blot analysis. Incubation with the proteasomal inhibitor MG132 was done in separate tubes. Quantification of western blot signals was done using ImageJ software (Schneider et al., 2012).

4.6 | mRNA isolation and RT-qPCR analysis

Total Arabidopsis RNA was isolated according to the manufacturer's protocol using an Isolate RNA Minikit (Bioline, NJ). cDNA was synthesized using a high-capacity DNA reverse transcription kit (Applied Biosystems, CA). RT-qPCR reactions were done using a 7500 Fast Real-Time PCR system (Applied Biosystems, CA) as described earlier (Mooney et al., 2019). Arabidopsis *Actin2* (*At3g18780*) was used as the internal control gene, and all experiments were repeated at least three times as biological replicates, if not otherwise stated. For *in planta* detection of *U-PEST* and *U-SBC* expression specific primer pairs were designed that covered eK and PEST or SBC regions, respectively. All primers used are listed in Table S1. The 2(-Delta Delta C(T)) method was used to calculate relative gene expression (Livak & Schmittgen, 2001).

4.7 | Statistical analysis

In all cases, Student's *t*-tests (heteroscedastic, two-tailed distribution) were performed using Microsoft Excel software. Values with $p < .05$ were considered significant. Error bars show standard deviations. If not otherwise stated, all calculated data are based on at least three biological replicates.

CONFLICTS OF INTEREST

The authors declare that there are no conflicts of interest.

AUTHOR CONTRIBUTIONS

R.A.-S. did the majority of the research work shown. S.M. particpated in plant phenotyping and RT-qPCR analysis. H.H. together with N.D. designed the U-PEST and U-SBC systems. All authors contributed in writing and editing the manuscript.

DATA AVAILABILITY STATEMENT

Primer and any additional data sets are available in supplemental materials.

ORCID

Nico Dissmeyer https://orcid.org/0000-0002-4156-3761
Hanjo Hellmann https://orcid.org/0000-0003-2177-2168

REFERENCES

Bachmair, A., Finley, D., & Varshavsky, A. (1986). In vivo half-life of a protein is a function of its amino-terminal residue. *Science*, *234*, 179–186. https://doi.org/10.1126/science.3018930

Bachmair, A., & Varshavsky, A. (1989). The degradation signal in a short-lived protein. *Cell*, *56*, 1019–1032. https://doi.org/10.1016/0092-8674(89)90635-1

Beathard, C., Mooney, S., Al-Saharin, R., Goyer, A., & Hellmann, H. (2021). Characterization of Arabidopsis thaliana R2R3 S23 MYB transcription factors as novel targets of the ubiquitin proteasome-pathway and regulators of salt stress and abscisic acid response. *Frontiers in Plant Science*, *12*, 629208. https://doi.org/10.3389/fpls.2021.629208

Belizario, J. E., Alves, J., Garay-Malpartida, M., & Occhiucci, J. M. (2008). Coupling caspase cleavage and proteasomal degradation of proteins carrying PEST motif. *Current Protein and Peptide Science*, *9*, 210–220. https://doi.org/10.2174/138920308784534023

Bernhardt, A., Lechner, E., Hano, P., Schade, V., Dieterle, M., Anders, M., Dubin, M. J., Benvenuto, G., Bowler, C., Genschik, P., & Hellmann, H. (2006). CUL4 associates with DDB1 and DET1 and its downregulation affects diverse aspects of development in Arabidopsis thaliana. *The Plant Journal*, *47*, 591–603. https://doi.org/10.1111/j.1365-313X.2006.02810.x

Bihmidine, S., Lin, J., Stone, J. M., Awada, T., Specht, J. E., & Clemente, T. E. (2013). Activity of the Arabidopsis RD29A and RD29B promoter elements in soybean under water stress. *Planta*, *237*, 55–64. https://doi.org/10.1007/s00425-012-1740-9

Carlsbecker, A., Lee, J.-Y., Roberts, C. J., Dettmer, J., Lehesranta, S., Zhou, J., Lindgren, O., Moreno-Risueno, M. A., Vatén, A., Thitamadee, S., Campilho, A., Sebastian, J., Bowman, J. L., Helariutta, Y., & Benfey, P. N. (2010). Cell signalling by microRNA165/6 directs gene dose-dependent root cell fate. *Nature*, *465*, 316–321. https://doi.org/10.1038/nature08977

Chen, L., Bernhardt, A., Lee, J., & Hellmann, H. (2015). Identification of Arabidopsis MYB56 as a novel substrate for CRL3(BPM) E3 ligases. *Molecular Plant*, *8*, 242–250. https://doi.org/10.1016/j.molp.2014.10.004

Chen, L., & Hellmann, H. (2013). Plant E3 ligases: Flexible enzymes in a sessile world. *Molecular Plant*, *6*, 1388–1404. https://doi.org/10.1093/mp/sst005

Chen, L., Lee, J. H., Weber, H., Tohge, T., Witt, S., Roje, S., Fernie, A. R., & Hellmann, H. (2013). Arabidopsis BPM proteins function as substrate adaptors to a cullin3-based E3 ligase to affect fatty acid metabolism in plants. *Plant Cell*, *25*, 2253–2264. https://doi.org/10.1105/tpc.112.107292

Chico, J. M., Lechner, E., Fernandez-Barbero, G., Canibano, E., Garcia-Casado, G., Franco-Zorrilla, J. M., Hammann, P., Zamarreno, A. M., Garcia-Mina, J. M., Rubio, V., Genschik, P., & Solano, R. (2020). CUL3 (BPM) E3 ubiquitin ligases regulate MYC2, MYC3, and MYC4 stability and JA responses. *Proceedings of the National Academy of Sciences of the United States of America*, *117*, 6205–6215. https://doi.org/10.1073/pnas.1912199117

Chitwood, D. H., Fabio, T. S., Nogueira, F. T. S., Howell, M. D., Montgomery, T. A., Carrington, J. C., & Timmermans, M. C. P. (2009). Pattern formation via small RNA mobility. *Genes & Development*, *23*, 549–554. https://doi.org/10.1101/gad.1770009

Choi, C. M., Gray, W. M., Mooney, S., & Hellmann, H. (2014). Composition, roles, and regulation of cullin-based ubiquitin e3 ligases. *Arabidopsis Book*, *12*, e0175. https://doi.org/10.1199/tab.0175

Clough, S. J., & Bent, A. F. (1998). Floral dip: A simplified method for agrobacterium-mediated transformation of Arabidopsis thaliana. *The Plant Journal*, *16*, 735–743. https://doi.org/10.1046/j.1365-313x.1998.00343.x

Curtis, M. D., & Grossniklaus, U. (2003). A gateway cloning vector set for high-throughput functional analysis of genes in planta. *Plant Physiology*, *133*, 462–469. https://doi.org/10.1104/pp.103.027979

Dissmeyer, N. (2017). Conditional modulation of biological processes by low-temperature Degrons. *Methods in Molecular Biology*, *1669*, 407–416. https://doi.org/10.1007/978-1-4939-7286-9_30

Dissmeyer, N. (2019). Conditional protein function via N-Degron pathway-mediated Proteostasis in stress physiology. *Annual Review of Plant Biology*, *70*, 83–117. https://doi.org/10.1146/annurev-arplant-050718-095937

Donde, R., Gupta, M. K., Gouda, G., Kumar, J., Vadde, R., Sahoo, K. K., Dash, S. K., & Behera, L. (2019). Computational characterization of structural and functional roles of DREB1A, DREB1B and DREB1C in enhancing cold tolerance in rice plant. *Amino Acids*, *51*, 839–853. https://doi.org/10.1007/s00726-019-02727-0

Dong, H., Dumenil, J., Lu, F. H., Na, L., Vanhaeren, H., Naumann, C., Klecker, M., Prior, R., Smith, C., McKenzie, N., Saalbach, G., Chen, L., Xia, T., Gonzalez, N., Seguela, M., Inze, D., Dissmeyer, N., Li, Y., & Bevan, M. W. (2017). Ubiquitylation activates a peptidase that promotes cleavage and destabilization of its activating E3 ligases and diverse growth regulatory proteins to limit cell proliferation in Arabidopsis. *Genes & Development*, *31*, 197–208. https://doi.org/10.1101/gad.292235.116

Faden, F., Mielke, S., & Dissmeyer, N. (2019). Modulating protein stability to switch toxic protein function on and off in living cells. *Plant Physiology*, *179*, 929–942. https://doi.org/10.1104/pp.18.01215

Faden, F., Mielke, S., Lange, D., & Dissmeyer, N. (2014). Generic tools for conditionally altering protein abundance and phenotypes on demand. *Biological Chemistry*, *395*, 737–762. https://doi.org/10.1515/hsz-2014-0160

Faden, F., Ramezani, T., Mielke, S., Almudi, I., Nairz, K., Froehlich, M. S., Hockendorff, J., Brandt, W., Hoehenwarter, W., Dohmen, R. J., Schnittger, A., & Dissmeyer, N. (2016). Phenotypes on demand via switchable target protein degradation in multicellular organisms. *Nature Communications*, *7*, 12202. https://doi.org/10.1038/ncomms12202

Figueroa, P., Gusmaroli, G., Serino, G., Habashi, J., Ma, L., Shen, Y., Feng, S., Bostick, M., Callis, J., Hellmann, H., & Deng, X. W. (2005). Arabidopsis has two redundant Cullin3 proteins that are essential for embryo development and that interact with RBX1 and BTB proteins to form multisubunit E3 ubiquitin ligase complexes in vivo. *Plant Cell*, *17*, 1180–1195. https://doi.org/10.1105/tpc.105.031989

Figueroa-Yanez, L., Pereira-Santana, A., Arroyo-Herrera, A., Rodriguez-Corona, U., Sanchez-Teyer, F., Espadas-Alcocer, J., Espadas-Gil, F., Barredo-Pool, F., Castano, E., & Rodriguez-Zapata, L. C. (2016). RAP2.4a is transported through the phloem to regulate cold and heat tolerance in papaya tree (*Carica papaya* cv. Maradol): Implications for protection against abiotic stress. *PLoS ONE*, *11*, e0165030. https://doi.org/10.1371/journal.pone.0165030

Focks, N., & Benning, C. (1998). wrinkled1: A novel, low-seed-oil mutant of Arabidopsis with a deficiency in the seed-specific regulation of carbohydrate metabolism. *Plant Physiology*, *118*, 91–101. https://doi.org/10.1104/pp.118.1.91

Gingerich, D. J., Hanada, K., Shiu, S. H., & Vierstra, R. D. (2007). Large-scale, lineage-specific expansion of a bric-a-brac/tramtrack/broad complex ubiquitin-ligase gene family in rice. *Plant Cell*, *19*, 2329–2348. https://doi.org/10.1105/tpc.107.051300

Johnson, E. S., Bartel, B., Seufert, W., & Varshavsky, A. (1992). Ubiquitin as a degradation signal. *The EMBO Journal*, *11*, 497–505. https://doi.org/10.1002/j.1460-2075.1992.tb05080.x

Julian, J., Coego, A., Lozano-Juste, J., Lechner, E., Wu, Q., Zhang, X., Merilo, E., Belda-Palazon, B., Park, S. Y., Cutler, S. R., An, C., Genschik, P., & Rodriguez, P. L. (2019). The MATH-BTB BPM3 and BPM5 subunits of Cullin3-RING E3 ubiquitin ligases target PP2CA and other clade a PP2Cs for degradation. *Proceedings of the National Academy of Sciences of the United States of America*, *116*, 15725–15734. https://doi.org/10.1073/pnas.1908677116

Krol, J., Busskamp, V., Markiewicz, I., Stadler, M. B., Ribi, S., Richter, J., Duebel, J., Bicker, S., Fehling, H. J., Schubeler, D., Oertner, T. G., Schratt, G., Bibel, M., Roska, B., & Filipowicz, W. (2010). Characterizing light-regulated retinal microRNAs reveals rapid turnover as a common property of neuronal microRNAs. *Cell*, *141*, 618–631. https://doi.org/10.1016/j.cell.2010.03.039

Lechner, E., Leonhardt, N., Eisler, H., Parmentier, Y., Alioua, M., Jacquet, H., Leung, J., & Genschik, P. (2011). MATH/BTB CRL3 receptors target the homeodomain-leucine zipper ATHB6 to modulate abscisic acid signaling. *Developmental Cell*, *21*, 1116–1128. https://doi.org/10.1016/j.devcel.2011.10.018

Livak, K. J., & Schmittgen, T. D. (2001). Analysis of relative gene expression data using real-time quantitative PCR and the 2(-Delta Delta C(T)) method. *Methods*, *25*, 402–408. https://doi.org/10.1006/meth.2001.1262

Ma, W., Kong, Q., Grix, M., Mantyla, J. J., Yang, Y., Benning, C., & Ohlrogge, J. B. (2015). Deletion of a C-terminal intrinsically disordered region of WRINKLED1 affects its stability and enhances oil accumulation in Arabidopsis. *The Plant Journal*, *83*, 864–874. https://doi.org/10.1111/tpj.12933

Maruyama, K., Sakuma, Y., Kasuga, M., Ito, Y., Seki, M., Goda, H., Shimada, Y., Yoshida, S., Shinozaki, K., & Yamaguchi-Shinozaki, K. (2004). Identification of cold-inducible downstream genes of the Arabidopsis DREB1A/CBF3 transcriptional factor using two microarray systems. *The Plant Journal*, *38*, 982–993. https://doi.org/10.1111/j.1365-313X.2004.02100.x

Mooney, S., Al-Saharin, R., Choi, C. M., Tucker, K., Beathard, C., & Hellmann, H. A. (2019). Characterization of Brassica rapa RAP2.4-related proteins in stress response and as CUL3-dependent E3 ligase substrates. *Cells*, *8*(4), 336. https://doi.org/10.3390/cells8040336

Morimoto, K., Ohama, N., Kidokoro, S., Mizoi, J., Takahashi, F., Todaka, D., Mogami, J., Sato, H., Qin, F., Kim, J. S., Fukao, Y., Fujiwara, M., Shinozaki, K., & Yamaguchi-Shinozaki, K. (2017). BPM-CUL3 E3 ligase modulates thermotolerance by facilitating negative regulatory domain-mediated degradation of DREB2A in Arabidopsis. *Proceedings of the National Academy of Sciences of the United States of America*, *114*, E8528–E8536. https://doi.org/10.1073/pnas.1704189114

Mot, A. C., Prell, E., Klecker, M., Naumann, C., Faden, F., Westermann, B., & Dissmeyer, N. (2018). Real-time detection of N-end rule-mediated ubiquitination via fluorescently labeled substrate probes. *The New Phytologist*, *217*, 613–624. https://doi.org/10.1111/nph.14497

Naumann, C., Mot, A. C., & Dissmeyer, N. (2016). Generation of artificial N-end rule substrate proteins in vivo and in vitro. *Methods in Molecular Biology*, *1450*, 55–83. https://doi.org/10.1007/978-1-4939-3759-2_6

Paturi, S., & Deshmukh, M. V. (2021). A glimpse of "dicer biology" through the structural and functional perspective. *Frontiers in Molecular Biosciences*, *8*, 643657. https://doi.org/10.3389/fmolb.2021.643657

Phuong, N. D., & Hoi, P. X. (2015). Isolation and characterization of a OsRap2.4A transcription factor and its expression in Arabidopsis for enhancing high salt and drought tolerance. *Current Science India*, *108*, 51–62.

Reichholf, B., Herzog, V. A., Fasching, N., Manzenreither, R. A., Sowemimo, I., & Ameres, S. L. (2019). Time-resolved small RNA sequencing unravels the molecular principles of microRNA homeostasis. *Molecular Cell*, *75*, 756–768. https://doi.org/10.1016/j.molcel.2019.06.018

Rissland, O. S., Hong, S.-J., & Bartel, D. P. (2011). MicroRNA destabilization enables dynamic regulation of the miR-16 family in response to cell-cycle changes. *Molecular Cell*, *43*, 993–1004. https://doi.org/10.1016/j.molcel.2011.08.021

Sakuma, Y., Maruyama, K., Osakabe, Y., Qin, F., Seki, M., Shinozaki, K., & Yamaguchi-Shinozaki, K. (2006). Functional analysis of an Arabidopsis transcription factor, DREB2A, involved in drought-responsive gene expression. *Plant Cell*, *18*, 1292–1309. https://doi.org/10.1105/tpc.105.035881

Schneider, C. A., Rasband, W. S., & Eliceiri, K. W. (2012). NIH image to ImageJ: 25 years of image analysis. *Nature Methods*, *9*, 671–675. https://doi.org/10.1038/nmeth.2089

Song, Y. H., Ito, S., & Imaizumi, T. (2013). Flowering time regulation: Photoperiod- and temperature-sensing in leaves. *Trends in Plant Science*, *18*, 575–583. https://doi.org/10.1016/j.tplants.2013.05.003

van Rooij, E., Sutherland, L. B., Qi, X., Richardson, J. A., Hill, J., & Olson, E. N. (2007). Control of stress-dependent cardiac growth and gene expression by amicroRNA. *Science*, *316*, 575–579. https://doi.org/10.1126/science.1139089

Varshavsky, A., Bachmair, A., Finley, D., Gonda, D. K., & Wunning, I. (1989). Targeting of proteins for degradation. *Biotechnology*, *13*, 109–143.

Vilarrasa-Blasi, J., Gonzalez-Garcia, M. P., Frigola, D., Fabregas, N., Alexiou, K. G., Lopez-Bigas, N., Rivas, S., Jauneau, A., Lohmann, J. U., Benfey, P. N., Ibanes, M., & Cano-Delgado, A. I. (2014). Regulation of plant stem cell quiescence by a brassinosteroid signaling module. *Developmental Cell*, *30*, 36–47. https://doi.org/10.1016/j.devcel.2014.05.020

Weber, H., Bernhardt, A., Dieterle, M., Hano, P., Mutlu, A., Estelle, M., Genschik, P., & Hellmann, H. (2005). Arabidopsis AtCUL3a and AtCUL3b form complexes with members of the BTB/POZ-MATH protein family. *Plant Physiology*, *137*, 83–93. https://doi.org/10.1104/pp.104.052654

Weber, H., & Hellmann, H. (2009). Arabidopsis thaliana BTB/POZ-MATH proteins interact with members of the ERF/AP2 transcription factor family. *The FEBS Journal*, *276*, 6624–6635. https://doi.org/10.1111/j.1742-4658.2009.07373.x

Wu, J., Yang, J., Cho, W. C., & Zheng, Y. (2020). Argonaute proteins: Structural features, functions and emerging roles. *Journal of Advanced Research*, *24*, 317–324. https://doi.org/10.1016/j.jare.2020.04.017

Zhang, Y., Liang, W., Shi, J., Xu, J., & Zhang, D. (2013). MYB56 encoding a R2R3 MYB transcription factor regulates seed size in Arabidopsis thaliana. *Journal of Integrative Plant Biology*, *55*, 1166–1178. https://doi.org/10.1111/jipb.12094

Zhuang, M., Calabrese, M. F., Liu, J., Waddell, M. B., Nourse, A., Hammel, M., Miller, D. J., Walden, H., Duda, D. M., Seyedin, S. N., Hoggard, T., Harper, J. W., White, K. P., & Schulman, B. A. (2009). Structures of SPOP-substrate complexes: Insights into molecular architectures of BTB-Cul3 ubiquitin ligases. *Molecular Cell*, *36*, 39–50. https://doi.org/10.1016/j.molcel.2009.09.022

SUPPORTING INFORMATION

Additional supporting information can be found online in the Supporting Information section at the end of this article.